

# A Novel Multi-Layer Beam Mechanism for Variable Stiffness Robotic Arms

Freddy Caro, Marc G. Carmichael

University of Technology Sydney

FreddySantiago.CaroDiaz@student.uts.edu.au

## Abstract

A stiff robot arm could cause significant injuries to human beings in the case of a collision. Introducing mechanical compliance into robots mitigates the effects of the impact and generates a safe interaction with human beings. An approach to modulating the stiffness of members in a robotic arm is the Multi-Layer Beam (MLB), which has a significant potential to achieve high stiffness variation and can be manufactured using traditional machining processes. In this paper, a new lock/unlock mechanism for the MLB has been proposed. It consists of a pneumatic actuator that drives a conical pin to interfere mechanically with the layers, and in turn changing the stiffness of the MLB. The conical pin mechanism was investigated by conducting experiments and Finite Element (FE) simulations. Both experiments and simulations show that this mechanism is able to increase the MLB stiffness by around 3.12 times. In addition, the effect of frames that surround the MLB was studied through FE simulations, showing that the increment of the number of frames rises the average of the stiffness range of the MLB and the stiffness ratio up to 11.5%.

## 1 Introduction

Numerous technologies have been studied to vary the stiffness of members in the robotic fields of Soft Robotics [Manti *et al.*, 2016] and Medical Devices [Blanc *et al.*, 2017]. The Multi-Layer Beam (MLB) is one of these technologies that has been investigated since 2002 [Kawamura *et al.*, 2002]. The MLB consists of a beam made of thin sheets and a mechanism to lock/unlock the sheets.

This article presents a novel mechanism to lock/unlock a MLB. Details of its design and manufacturing are ex-

plained. It also presents the experiments and Finite Element Simulations that were conducted to evaluate its capacity to variate the stiffness of a robot link arm. The effect of number of *frames* surrounding the MLB was also investigated through FE simulations. Finally, future developments of this mechanism are proposed.

### 1.1 Motivation

In the last 10 years, collaborative robots that can work alongside humans have come to market. From this has arisen a set of problems about how robots and human interact. One of these problems is the reduction of damage during an impact between a human being and a robot. This problem is critical because Human beings could suffer serious or even fatal injuries if they received a rigid impact from a robot. In addition, the impact could cause serious damage to the mechanical adjustment of the robot. A practical solution to reduce the risk is for manipulators to have mechanical compliance.

The mechanical compliance in robots can be implemented through two approaches. Variable Stiffness Joints (VSJ) and Variable Stiffness Links (VSL). VSJ has been widely studied in human robot interaction by [Albu-Schaffer *et al.*, 2008; Petit *et al.*, 2010; Petit, 2014; Schiavi *et al.*, 2008]. VSL has been recently explored by [López-Martínez *et al.*, 2015; Park *et al.*, 2008; She, 2018]. A comparison of performance between VSJ and VSL robots in human-robot impact presented by [She, 2018] demonstrates that a VSL robot can generate lighter injuries than a VSJ robot for the same design parameters given.

The stiffness ratio is the ratio between the maximum stiffness and the minimum stiffness. It is an important indicator to evaluate the performance of Variable stiffness technologies. Some MLB technologies are adequate to change the stiffness of robot link arms because they can achieve stiffness ratios from 10 [Manti *et al.*, 2016] to 180 [Hurd, 2017; Zeng *et al.*, 2020]. In addition, these MLB mechanisms have high speeds of stiffening and des-tiffening [Manti *et al.*, 2016]. Furthermore, the majority of MLB technologies have the significant advantage of re-

quiring traditional and simple manufacturing processes such as machining or laser cutting that make it relatively easy to manufacture [Henke and Gerlach, 2014].

The existing mechanisms to lock/unlock the MLB are based on friction, mechanical interference, or miscellaneous principles. In general, they have demonstrated to be effective to achieve the variation of stiffness. However, the speed of stiffening and destiffening is still too slow to be applied in attenuation of an impact between a robot arm and a human being. For instance, laminar jamming is the lock/unlock mechanism with the highest speed of stiffening and destiffening. It has been applied as mechanism to change the stiffness of a haptic glove. The necessary time to change completely the stiffness of the haptic glove is characterized by a time constant about 0.5 seconds [Zubrycki and Granosik, 2016]. This time is much smaller than the typical time of stiffening and destiffening presented by [Henke and Gerlach, 2014] (hundreds of seconds). However, it is still too large considering that the damage due to impacts between industrial robotic arms and humans takes about 0.1 seconds [Albu-Schaffer *et al.*, 2008].

The new lock/unlock mechanism for MLB proposed in this article has the potential to achieve a rapid change from the rigid state to the flexible state in order to be useful during an impact between a human being and a robot link composed of a MLB with this mechanism.

## 2 Working Principle of Multilayer Beam

The MLB consists of a beam that is made of thin sheets and a mechanism to lock/unlock the sheets. All the MLBs have the same working principle independently of the lock/unlock mechanism. When the mechanism locks the sheets, the bending stiffness is high and the whole beam behaves similarly to a rigid member as can be seen in Figure 1a. When the mechanism unlocks the sheets, they can slide between them, the bending stiffness is low and the beam becomes flexible as can be observed in Figure 1b. In this state, the layers are not coupled and there is slip between them.

The stiffness ratio in a MLB depends on the number of layers raised to the 2nd power [Kawamura *et al.*, 2002; Henke and Gerlach, 2014]. This generates, at least in theory, the possibility of obtaining very high stiffness variation by only adding more layers to the beam [Henke and Gerlach, 2014]. However, this is a theoretical value because other factors, such as friction and efficacy of the lock/unlock mechanism, would reduce the stiffness ratio that can be achieved.

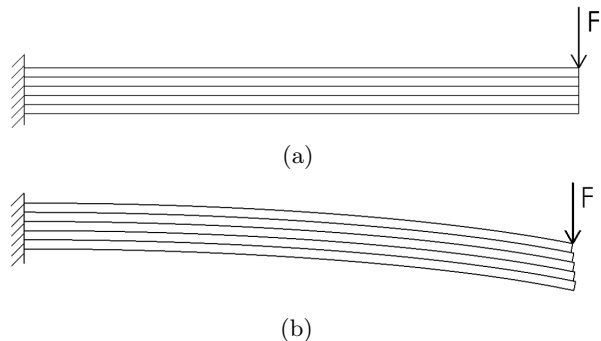


Figure 1: Variable Stiffness of the MLB in a) Rigid state b) Flexible state

## 3 Design and Analysis of Conical Pin Mechanism

### 3.1 Conical Pin Concept

The Multi-Layer Beam (MLB) that is presented in this article has a lock/unlock mechanism that is based in a combination of the principles of friction and mechanical interference. Figure 2 and Figure 3 show the components of this mechanism and the MLB. It consists of a conical pin that is coupled with the rod of a pneumatic cylinder. Figure 3b shows that when the cylinder is pressurised, the conical pin is thrust into a conic hole formed by the circular holes in the layers. The conical pin compresses the layers and increases the friction force between them in that area. The fact that the pin comes in and out of the MLB generates mechanical interference. When the conical pin is disengaged, the MLB has the lowest stiffness (Figure 3a). When the pin is engaged, the stiffness depends on the force that is applied to the pin, which in turn depends on the air pressure in the pneumatic cylinder (Figure 3b).

When the MLB is deformed by bending, the slip between the layers pushes the pin out due to its conical shape. This phenomenon facilitates a fast transition from a stiff state to a flexible state. In contrast, a straight pin or cylindrical pin, tends to get stuck by the layers when the MLB is bent as was observed in preliminary qualitative experiments.

The general characteristics of each component of the MLB are described as follows.

**Layers:** The presented MLB has 22 layers that are made of stainless steel shims with length of 350mm (300 mm for MLB length and 50mm for holding with C-clamp), width of 35mm, and thickness of 0.318mm. Each layer has a hole with a different diameter to accommodate the conic pin.

**Frames:** Frames are distributed along the beam to reduce layer buckling. The frames do not constrain the relative slipping of the layers due to a small clearance.

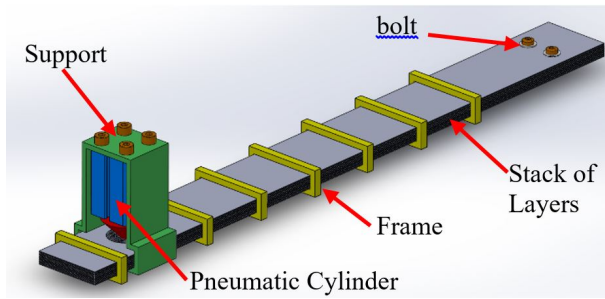


Figure 2: Proposed Lock/Unlock mechanism

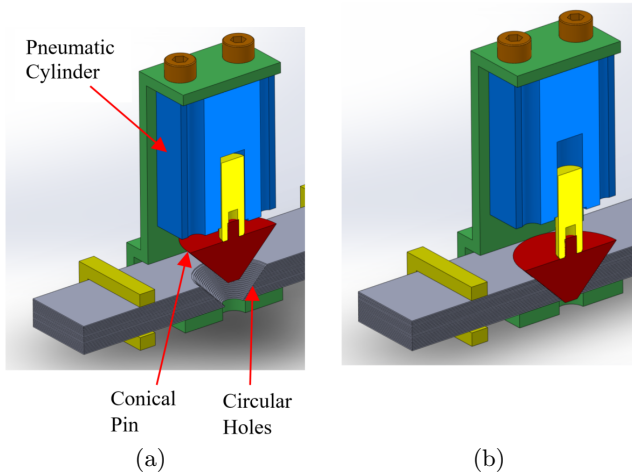


Figure 3: Longitudinal section of the mechanism when the pin is out of the MLB b) Longitudinal section of the MLB when the pin is in of the MLB

Some of the frames are bonded to the bottom layers and others to the top layer, but none are bonded to both.

**Support of Pneumatic Cylinder:** This part is bonded to the bottom layer and has enough height to allow the conical pin to come out completely from the MLB. Therefore, it does not constrain the slip between the layers.

**Pneumatic Cylinder(SMC- CDQSB12-10D):** This actuator was selected because its high force per weight output compared to other actuators such as solenoids.

**Conical Pin:** The conical pin was made of industrial nylon. The angle of the tip of the cone is 90 deg.

**Pneumatic circuit:** The pneumatic circuit has a 5/2 pneumatic valve with manual actuation that controls the motion of the cylinder rod. The circuit also has a pressure regulator that allows to control the pressure in the whole circuit including the pneumatic cylinder.

The proposed MLB can be used to build parallel guided beam links with variable stiffness capabilities in one direction, similar developments have been presented by [Hurd, 2017; Zeng *et al.*, 2020] This type VSL can be



Figure 4: Deflection of the layers due to the rolling shape of the raw material

useful in robotic arms whose links move in only one plane such as SCARA robots and planar 5 bar parallel robots. Furthermore, this type of links could be combined in robotic arms to generate variable stiffness capabilities in 3 axes as it is demonstrated by [She, 2018].

### 3.2 Manufacturing of the MLB

The layers are the components that require most work and attention. The raw material is a large sheet that comes in rolls. To cut the sheets of the MLB from this raw material, it is necessary to cut the roll in smaller rectangles and then place them in a laser cutting machine that cuts each layer of the MLB. The laser cutting process is accurate and it does not deform the sheets. However, it generates burrs on the edges of the sheets. These burrs are small but they were high enough to prevent the correct contact between the sheets. Therefore, it is necessary to deburr the edges with a pedestal grinder and a handheld grinding tool.

The fact that the raw sheet material comes in rolls generates a curved shape of the layers as illustrated in Figure 4.

### 3.3 Experiment set up

The purpose of the experiment was to determine the variation of stiffness of the MLB in function of the air pressure in the pneumatic cylinder. The experimental set up was completely assembled on the table of a vertical milling machine in order to take advantage of the high stiffness of its structure. A similar setup was used by [She, 2018] to carry out static experiments in VSLs. Figure 5 illustrates the components of the experimental set up. The force was measured by a YUTON HDM2006LS load cell that has a resolution of 0.019N and nonlinearity of 0.02%. The deflection was measured by height gauge with 0.02mm resolution.

### 3.4 Experimental Procedure

At the beginning of each test, the MLB is deflected by its own weight. This deflection prevent the correct accommodation of the conical pin in the circular holes of the MLB. In consequence, the MLB is not locked properly. To solve this problem, the MLB is manipulated manually to properly accommodate the conical pin in the holes of the MLB.

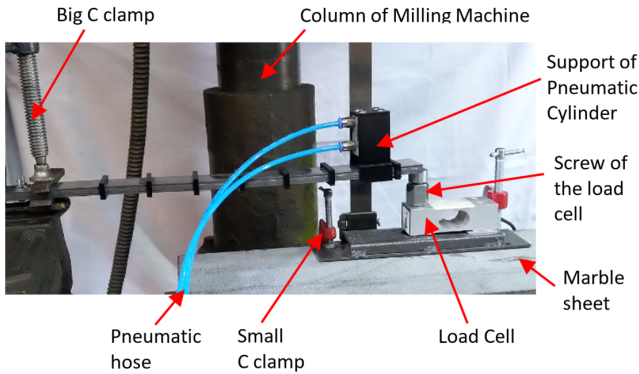


Figure 5: Experimental Set up

The procedure to generate the deflection of the MLB and measure the force is similar to the procedure presented by [Gandhi and Kang, 2007]. The deflection of the beam is generated through the manual rotation of the screw of the load cell. The contact force between the screw and the MLB is measured by the load cell. For every value of deflection, there is a corresponding value of force.

The force is measured every two revolutions of the screw which correspond to approximately 3 mm of axial motion of the screw. However, as there is not precise control of the manual rotation of the screw, the height gauge was used to measure the deflection of the free end of the beam. It is important to know that these values have to be recorded after the force has reached a stable value. For this reason, it can be considered that the MLB is loaded and unloaded quasi-statically. This type of static experiment is necessary before conducting dynamic tests and provide valuable inputs for dynamic models of on VSL composed of MLBs [Song *et al.*, 2019].

The experiment of force vs deflection consisted on the application of a complete load-unload cycle at 0, 2, 4, 6 and 7 bar of pressure in the pneumatic cylinder. The test begins with the loading procedure where the deflection increases from zero until reaching a maximum value about 30mm. Then, the unloading procedure begins by reducing the deflection until the straight position of the MLB, reaching a deflection very close to zero.

### 3.5 Results of Experiments

Figure 6 illustrates the results of this experiment for a locking pressure of 0 bar in pneumatic cylinder. The upper branch of the curve is the loading procedure. The lower branch of the curve represents the unloading procedure. Three trials were conducted at each pressure value. The points illustrated in the Figure 6 correspond to the average of the forces obtained in the 3 trials for a given deflection. The error is illustrated in the Figure 6 through the error bars that reflect the range of force values obtained across the 3 trials for a given deflection. A

similar procedure to illustrate the error in stiffness tests was implemented by [Gal, 2007].

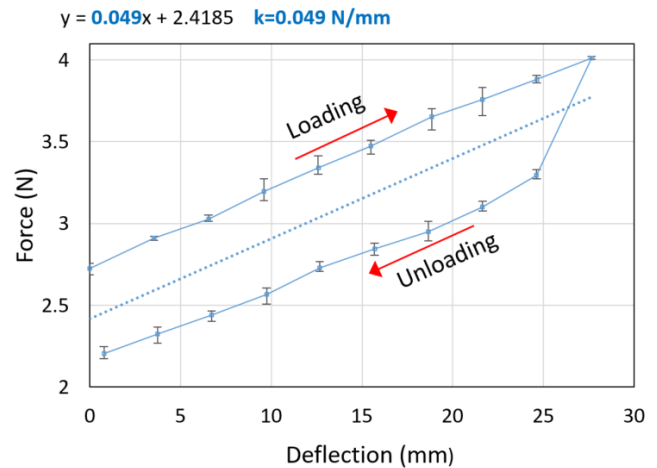


Figure 6: Results of the experiments at 0 bar

The stiffness of the MLB is the slope of the curve Force vs Deflection. Figure 6 and Figure 7 show hysteresis in the MLB which means that there is not a unique value of stiffness for a given pressure. This phenomenon is also reported by [Henke and Gerlach, 2014] and [Narang *et al.*, 2018].

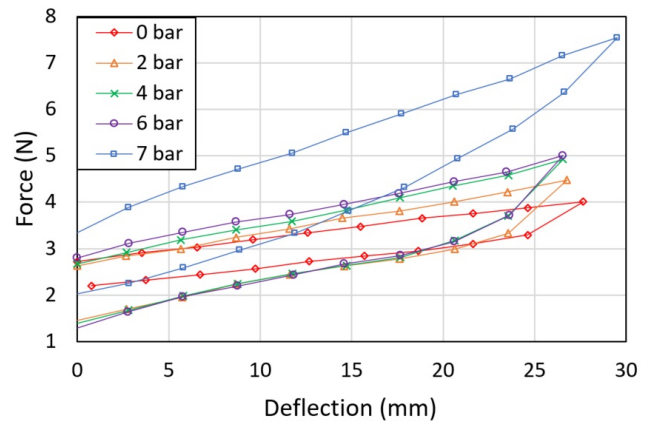


Figure 7: Results of the Experiments

In order to compare the stiffness of the MLB for different air pressures in the pneumatic cylinder, it is necessary to calculate a unique value of stiffness for each pressure. Therefore, following the same procedure that is applied by [Henke and Gerlach, 2014; Zhou *et al.*, 2019b]. The results of the experiment at each value of pressure were linearized by the method of least square which yields a straight line whose slope is the stiffness  $k$ . The linearization includes the loading and unloading data.

The Table 1 shows the stiffness calculated from the

Table 1: Stiffness for each state of air pressure in the pneumatic cylinder

Pressure (bar)	0	2	4	6	7
Stiffness (N/mm)	0.049	0.076	0.091	0.091	0.153

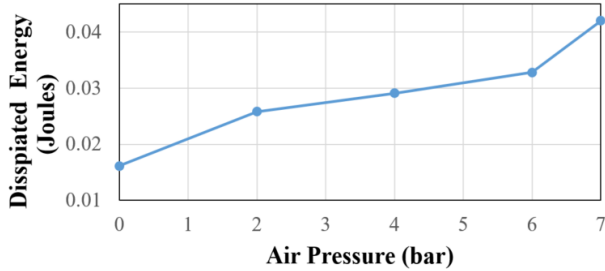


Figure 8: Energy dissipated in function of air pressure in the pneumatic cylinder

linearization of the results at each state of pressure in the pneumatic cylinder. It can be observed that the minimum stiffness is 0.049 N/mm and corresponds to 0 bar. The maximum stiffness, is 0.153 N/mm and corresponds to 7 bar. The stiffness ratio is calculated as the ratio between the maximum stiffness and the minimum stiffness, which yields 3.12 for this novel lock/unlock mechanism.

The calculation of stiffness from the experiments could be calculated through other methods. For example, the stiffness can be calculated only for the loading part of the cycle (the upper branch of the curve). This is the method adopted by [Gandhi and Kang, 2007; Kawamura *et al.*, 2002]. If we apply this method to the previous experimental results, the maximum stiffness ratio is 2.95. The difference with the value calculated by considering the complete load-unload cycle (3.12) is 5.4%.

### 3.6 Hysteresis and Energy Dissipation

The results show the presence of the hysteresis phenomenon in the MLB. The presence of hysteresis is likely due to the friction forces in the MLB. The friction force is a non-conservative force that dissipates energy during the loading cycle. The area under the hysteresis curve is equal to the energy dissipated over the loading cycle [Narang *et al.*, 2018] and can be used to quantify the hysteresis itself.

There are two sources of friction in this particular lock/unlock mechanism: the friction force between the layers, and the friction force between the conical pin and the layers. When the conical pin engages with the MLB, it produces a combination of two effects that lock the layers. One effect is the mechanical interference that opposes the shear slip between the layers. Another effect is the application of normal forces between the layers,

which increases the friction force in the area surrounding the holes that accommodate the conical pin.

At zero bar, there is no normal force due to the pin and the friction between the layers is low. As a result, the hysteresis at this pressure is lower than at other pressures as can be seen in the Figure 8. A similar result is present in the experiments conducted by [Henke and Gerlach, 2014]. Overall, hysteresis rises with pressure because of the normal force applied to the MLB, which in turns increases the friction force between the layers. It should be noted that the maximum deflection at 7 bar is 3 mm higher than for the rest of pressure values. Therefore, hysteresis at 7 bar is higher because of the increment in friction force and the additional deflection.

### 3.7 Discussion of Experimental Results

The proposed lock/unlock mechanism of the MLB achieves a stiffness ratio of 3.12. The measured stiffness ratio is much less than the theoretical maximum that could be achieved if all the MLB layers were joined to form one solid member (484 for  $N=22$ ) as it was explained in section 2. In this experiment, the maximum pressure that the air compressor can supply is 8 bar. If the air compressor can supply 10 bars, which is the operative limit of the pneumatic cylinder, the maximum stiffness ratio could be higher.

The locking mechanism presented in [Zhou *et al.*, 2019b] consists of clamps in the middle and the end of MLB, and is the most similar mechanism to the conical pin. It shows a stiffness ratio of 5 when only the end clamp is implemented. This mechanism exceeds the stiffness ratio of the conical pin (3.12). However, it is necessary take into account that the conical pin has a contact area with the layers that is smaller than the clamp mechanism. Therefore, the results of this experiment do not allow to definitely conclude that the conical pin is less effective than the clamp mechanism.

Table 1 and Figure 12 show a nonlinear relation between the stiffness of the MLB and the air pressure in the pneumatic cylinder. In general, it can be seen that the stiffness of the MLB increases with air pressure in the pneumatic cylinder, except in the range from 4 bar to 6 bar where the stiffness is almost constant. This nonlinear behaviour was unexpected. However, the experiments conducted by [Zhou *et al.*, 2019b] show a similar behaviour in the lock/unlock mechanism based on clamps placed along the MLB. Section 3.9 discusses some possible explanations for the constant stiffness between 4 and 6 bar in the proposed MLB.

### 3.8 Finite Element Simulation of the Conical Pin

MLBs with other lock/unlock mechanism have been modelled by analytical methods or finite element (FE)



methods in order to study the mechanical behaviour of the MLB with such mechanisms [Henke and Gerlach, 2016; Murray and Gandhi, 2010; Narang *et al.*, 2018; Zhou *et al.*, 2019b]. In the case of MLB with many layers, FE methods would be preferred over analytical methods because analytical methods are algebraically taxing [Narang *et al.*, 2018]. This section presents FE Simulations of the of MLB mechanism proposed in this study.

A finite element (FE) model was built in Ansys with the same dimensions and components as the experimental set up. The FE model has the same load and boundary conditions that were implemented in the experiment. These conditions are the following: the MLB model is fixed in one its ends; gravity force is considered; deflection is imposed at the free end following the same values that were imposed in the experiment; the pressure in the pneumatic cylinder is implemented as a pair of forces that are applied to the cylinder rod and the cylinder body, the value of these forces correspond to the forces applied by the cylinder when it is pressurized at the same values of pressure of the experiment (0 bar, 2 bar, 4 bar, 6 bar, 7 bar). The result of the simulation is the force associated with each value of the enforced deflection.

The most relevant details about the pre-process of the simulation are mentioned as follow: Only one half of the MLB sample is modeled and symmetry along the longitudinal plane was imposed as can be seen in Figure 9 and Figure 10. The mesh of the layers is composed of elements of quadratic order and all the layers have one element across the thickness. *Large deflection* is turned on considering that the maximum deflection in the experiment was about 10 % of the length of the beam. The set up of the contact among the layers, and between the layers and the pin had a determinant role in the convergence of the simulation. In this aspect, the most important parameters are the Contact Formulation which was selected as Augmented Lagrange, normal stiffness factor is set up as 0.01, and the stiffness is updated in each iteration.

Figure 9 illustrates the shape of the MLB at a locking pressure of 7 bar when it reaches the maximum deflection of the free end that was imposed in the experiment. It can be appreciated that the curvature of the MLB is very low in the section that is close to the conical pin mechanism. In other words, the action of the conical pin makes that section of the MLB straight.

Figure 10a shows some details that are not possible to observe in the experiment. It can be seen that the conical pin only keeps contact with some of the top layers in the rear of the pin and some of the bottom layers in front of the pin. Figure 10b shows the detail of one of the contact zones indicated in Figure 10a, it can be

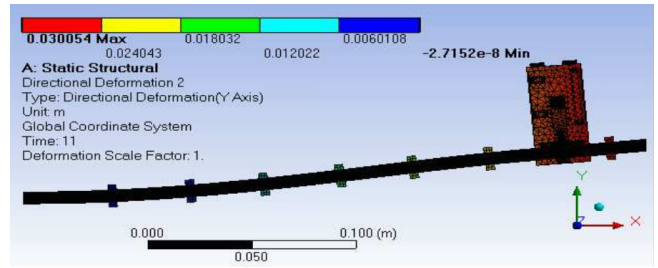
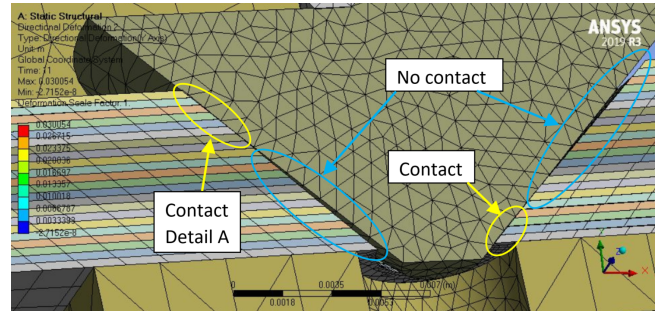


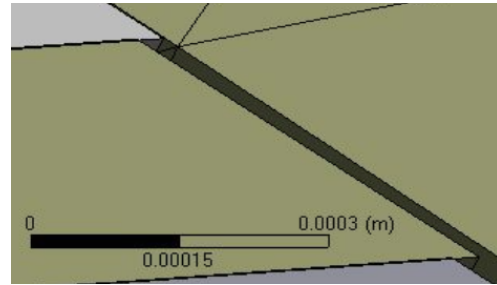
Figure 9: Resulting shape of MLB at 7 bar and COF 0.32 from FE simulation

appreciated how one layer is in contact with the conical pin while the layers below it are not in contact in the conical pin anymore. This Figure also illustrates the relative slip between the layers.

As it was mentioned in the section 3.1, the layers pushed the conical pin when the MLB bends. This displacement is about 0.16 mm for a deflection of about 30 mm of the free end.



(a)



(b)

Figure 10: Conical Pin Mechanism after deformation of MLB a) contact and no contact zones between conical Pin and the layers b) Detail A: transition from contact to no contact

### 3.9 Experiments Versus Simulations

Figure 11 illustrates the results of the FEM simulations and the experiment for the MLB at 7 bar and a coefficient of friction (COF) of 0.32. It can be observed that the simulation results agree with experimental results very well for the loading part of the cycle but differ sig-

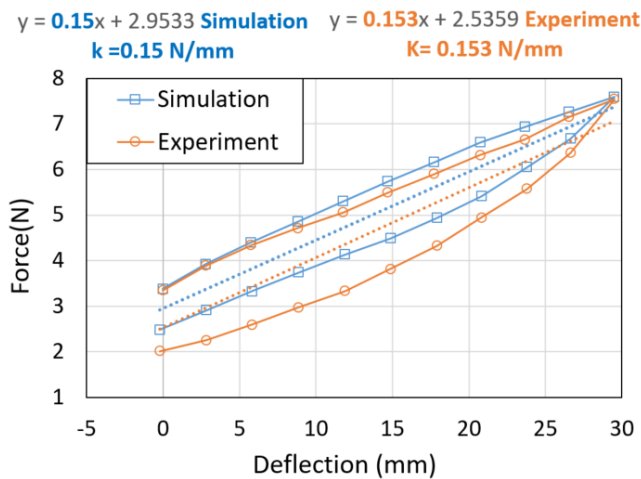


Figure 11: Force-Deflection curves for 7 bar pressure and COF 0.32 from FEM simulation and Experiment

nificantly in the unloading part of the cycle. Both results were linearized, which yields a stiffness of  $k=0.15$  N/mm in the simulation, and a stiffness of  $k=0.153$  N/mm in the experiment. It can be appreciated that the stiffness values of the simulation and the experiments were very close.

**Coefficient of Friction**

The coefficient of friction between the components of the MLBs is an important parameter in the MLB behaviour. Measuring the COF between the layers is a difficult task because of the curvature of the sheets and the lack of uniform surface finishing of the sheets that results from the elimination of burrs. Despite these difficulties, a first approach to define the COF among the layers was carried out by conducting some experiments. A sample of three pairs of layers were selected for these tests. The COF between the layers was measured by the method described by [Blau, 2008] which uses an inclined-plane friction apparatus. The same experiment was carried out between the layers and the conical Pin. The results of these experiments indicate that the COF between the layers is 0.39 and the COF between the layers and conical pin is 0.25.

Figure 12 compares the experimental and the simulation stiffnesses for all the pressure values that were tested in the experiment. The first set of FEM simulations were run with the COF values that resulted from the friction experiments (0.39 between the layers and 0.25 between the layers and the conical Pin). The results of these simulations agrees well with the experiment at 0 bar and 7 bar, but results differ considerably at 2 , 4, and 6 bar.

The differences between the simulation and the experiment at 2, 4, and 6 bar could be caused by the lack of uniform contact between the layers. As it was explained in the section 3.2, the sheets keep a curved shape due

to the manufacturing process of the raw material, when they are assembled in the MLB, the curvature of the sheets generates gaps between them which reduces the area of contact. As a consequence, the friction force between the layers decreases as well. Including this phenomenon in the FE simulation by altering the geometries of the sheets is very difficult since it would require to know where the gaps are with accuracy. Instead, the reduction of friction between the layers was simulated by reducing the COF to 0.32 and 0.25 as shown in Figure 12. It can be seen that the results of the FE simulations get closer to the results of the experiments at 2, 4, and 6 bar when the COF decreases. In particular, the result of the simulation with COF 0.25 agrees very well with the result of the experiment at 2 bar while the results at 0 bar and 7 bar remain close to the result of the experiment.

Figure 12 shows that change of stiffness for different values of COF is small at low pressure ( 0 bar) and high pressure(7 bar). These results match the results of the FE simulations carried out by [Zhou *et al.*, 2019b]. At low pressure, the friction force is small because the normal force between the layers is low. Therefore, the effect of variation in COF is not significant in the stiffness. At high pressure (7 bar), the best COF that fits the experimental results is 0.32 which suggest that this could be the actual average of COF between the layers of the MLB.

The difference between simulation and experimental results at 4 and 6 bar could have another explanation apart from the gaps between the sheets. As it was explained in the section 3.4, the experiment requires the manual accommodation of the conical pin in the holes of the MLB before each test. At 4 and 6 bar, the manual accommodation of the pin could not have been appropriate, which may have an effect in the stiffness of the beam at these pressures.

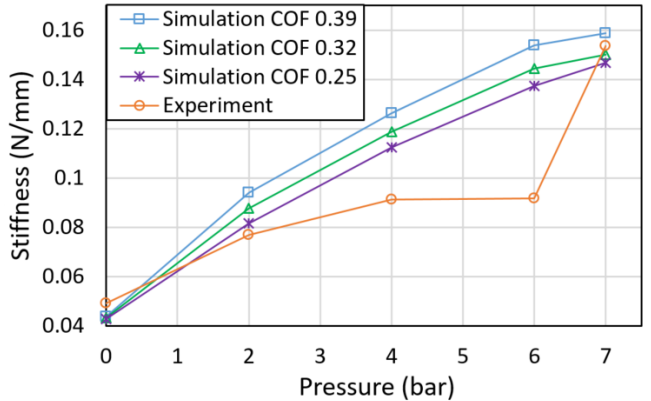


Figure 12: Comparison of stiffness from experiments and simulations with different COF between the layers

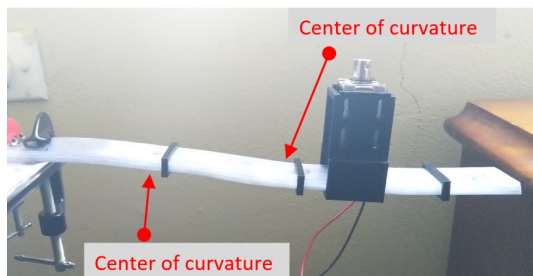


Figure 13: Curvature reversal in a MLB with conical pin

### Curvature Reversal

There is a notable difference between the deformed shape of a rigid cantilever beam and a MLB when they are under a uniform load or under a point load. The curvature of a rigid beam has a consistent sign. In contrast, the curvature of the MLB reverses along the beam, (i.e., changes its sign). For example, Figure 13 illustrates the change in curvature of a MLB whose layers are locked by a conical pin driven by a solenoid. Figure 9 and Figure 17b show that FE simulations are able to reproduce the curvature reversal in the proposed MLBs. This phenomenon has been reported in laminar jamming structures as well [Narang *et al.*, 2018].

## 4 Effect of frames in the MLB

The MLB proposed in this article has frames, which are a novel component in comparison with other MLB mechanisms. For this reason, this section focuses only in the study of the effect the number of frames in the MLB through FE simulations. The performance of the MLB also depends on other parameters such as the number of actuators, the location of the actuators and the number of layers. These parameters were not included in this research because they have been extensively investigated by [Zhou *et al.*, 2019b] in discrete laminar jamming. The conclusions from that study can be applied to the conical pin mechanism because both mechanism shares the concept of discrete actuators placed in specific locations of the MLB.

In addition to the variation of the number of frames. The conical pin was replaced by a trapezoidal pin as can be seen in Figure 14. Both shapes of the pin work similarly, but the trapezoidal pin keeps contact with the layers along the width of the pin as the MLB is deflected, which is a more favorable contact condition in comparison with the conical pin that keeps contact with the layers only in one point as the MLB bends.

To validate the configuration of the parameters used in the FE simulation. The laminar jamming structure presented by [Zhou *et al.*, 2019b] was also simulated in Ansys but using the parameters described in the section 3.8. As can be seen in Figure 15, the results of the simu-

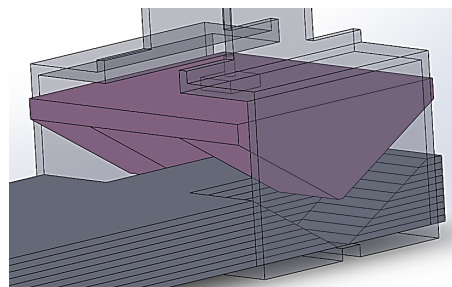


Figure 14: Trapezoidal pin with 120deg at the tip

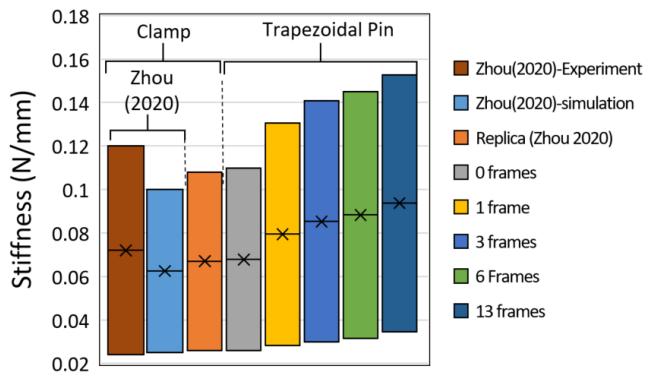


Figure 15: Comparison of stiffness range of the MLB for different number of frames

lation in Ansys have 4% error for the minimum stiffness, and 8% error for the maximum stiffness in relation with the simulations presented by [Zhou *et al.*, 2019b].

FE simulations were carried out in an MLB with a trapezoidal pin at the free end and with 0, 1, 3, 6 and 13 frames distributed along the MLB. The dimensions, materials and load conditions are the same as the laminar jamming presented by [Zhou *et al.*, 2019b]. The rest of the simulation parameters are the same that were described in section 3.8.

For each number of frames, the simulations were run at 0 bar and 10 bar of pressure in the pneumatic cylinder to calculate the minimum and maximum stiffness respectively. The results are presented in the Figure 15. It can be appreciated that the main effect of the number of frames is the displacement of the stiffness range of the MLB, as the number of frames grows, the minimum, the maximum, and the average values of stiffness increases. For instance, the comparison of the stiffness range between 0 frames and 13 frames, shows that there is an increment of 39.3% in the maximum stiffness and 33.6% in the minimum stiffness.

Figure 16 illustrates the behaviour of the stiffness ratio in function of the number of frames. The maximum stiffness ratio happens when there are 3 frames in the MLB and represents an increment of about 11.3% in



relation with the minimum stiffness ratio that happens when there is not any frame. Figure 15 and Figure 16 indicate that increasing the number of frames beyond 3 frames increases the stiffness average of the MLB but reduces its stiffness ratio.

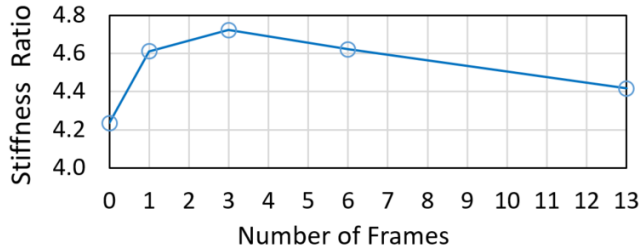


Figure 16: Stiffness Ratio in function of the number of frames

Frames prevent the buckling of the layers when the MLB is bent by transversal forces as can be observed in Figure 17. When there is not any frame, the layers buckle as transversal load is applied and deforms the MLB. Since the layers do not have any restriction and the trapezoidal pin opposes the relative slip between the layers at the free end, the layers buckle independently and lost contact between them (Figure 17a). When there are frames in the middle of the MLB, these frames keep the layers together in the corresponding section of the beam, resulting in a significant reduction of the buckling of the layers as can be observed in Figure 17b.

The manipulation of the stiffness range of the MLB by changing the number of frames offers two advantages. First, frames are passive elements that do not require any actuator to be effective. Second, it is a very practical method that does not require the total disassembly of the MLB. In the context of the use of the MLB in a cobot, this method will allow the change of stiffness range without interrupting the operation of the cobot for long periods of time. In addition. The implementation of frames is also possible in MLBs with other lock/unlock mechanisms such as clamps [Zhou *et al.*, 2019b] and shape memory alloy wires [Henke and Gerlach, 2014].

## 5 Conclusion and Future Work

This paper has introduced a locking mechanism for MLBs based on a conical pin. The concept of the mechanism, experiments, and FE simulation were presented. Overall, both experiments and simulations verified that bending stiffness increases with pressure in the pneumatic cylinder that drives the conical pin.

Experiments and simulation results agree for low and high pressures but do not match at medium pressures. These difference may be caused by defects in the manufacturing of the raw material of the sheets, and possible

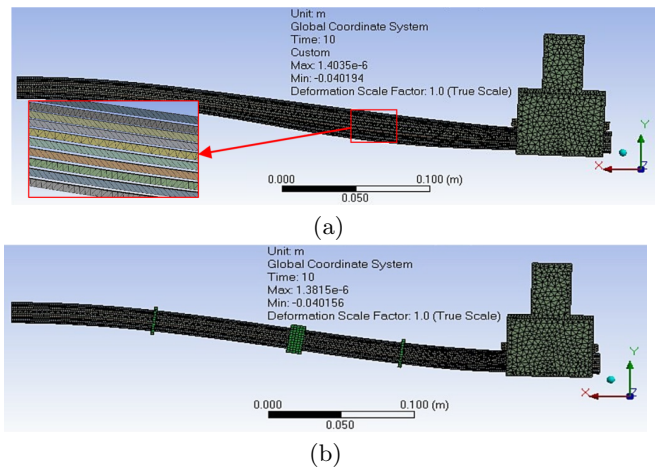


Figure 17: Deflection in Y axis. a) MLB with no frames b) MLB with three frames

errors in the experimental procedure at medium values of pressure.

The effect of the number of frames in combination with a trapezoidal pin was investigated through FE simulations, which show that the increase of the number of frames generates the rise of the average of the stiffness range. In addition, the stiffness ratio reaches a maximum value when there are 3 frames in the MLB, showing an increment of about 11.5% in relation with the minimum stiffness ratio. Overall, changing the number of frames is a novel and practical method to manipulate the range of stiffness without adding more actuators to the MLB.

Future work should focus on fundamental aspects such as analytical models of stiffness of MLBs with trapezoidal pin and frames. The angle at the tip of the trapezoidal pin should be also investigated through FE simulations to determine its effect in the stiffness of the MLB. The deformed shape of the MLB must be measured in future experiments because it can be useful for the development of forward kinematics models and dynamic models of a link made of MLBs.

The speed of actuation must be determined in order to define if pneumatic circuits are fast enough to be useful in the mitigation of impact between human beings and robots. In addition, other types of actuators could be implemented to drive the conical pin such as piezoelectric actuators since the speed of the actuation could be improved. For future developments, it is recommended to use metallic sheets for the MLB only if they are completely flat, in order to avoid gaps between the layers when they form the MLB and the subsequent reduction in friction force between the layers.

## 6 Acknowledgments

This research is supported by an Australian Government Research Training Program (RTP) Scholarship.

The authors would like to thank LEAP Australia for its technical support in the development of Simulations in Ansys.

## References

- [Albu-Schaffer *et al.*, 2008] Alin Albu-Schaffer, Oliver Eiberger, Markus Grebenstein, Sami Haddadin, Christian Ott, Thomas Wimbock, Sebastian Wolf, and Gerd Hirzinger. Soft robotics. *IEEE Robotics Automation Magazine*, 15(3):20–30, 2008.
- [Blanc *et al.*, 2017] Loïc Blanc, Alain Delchambre, and Pierre Lambert. Flexible medical devices: Review of controllable stiffness solutions. *Actuators*, 6(3):23, 2017.
- [Blau, 2008] P.J. Blau. *Friction Science and Technology: From Concepts to Applications, Second Edition*. Mechanical Engineering. CRC Press, 2008.
- [Gal, 2007] *Design of a Multi-Directional Variable Stiffness Leg for Dynamic Running*, volume Volume 10: Mechanics of Solids and Structures, Parts A and B of *ASME International Mechanical Engineering Congress and Exposition*, 11 2007.
- [Gandhi and Kang, 2007] Farhan Gandhi and Sang-Guk Kang. Beams with controllable flexural stiffness. *Smart Materials and Structures*, 16(4):1179–1184, 2007.
- [Henke and Gerlach, 2014] Markus Henke and Gerald Gerlach. On a high-potential variable-stiffness device. *Microsystem Technologies*, 20(4):599–606, 2014.
- [Henke and Gerlach, 2016] M Henke and G Gerlach. A multi-layered variable stiffness device based on smart form closure actuators. *Journal of Intelligent Material Systems and Structures*, 27(3):375–383, 2016.
- [Hurd, 2017] Carter Hurd. *Variable stiffness robotic arm for safe human-robot interaction using layer jamming*. PhD thesis, The Ohio State University, 2017.
- [Kawamura *et al.*, 2002] S. Kawamura, T. Yamamoto, D. Ishida, T. Ogata, Y. Nakayama, O. Tabata, and S. Sugiyama. Development of passive elements with variable mechanical impedance for wearable robots. In *Proceedings 2002 IEEE International Conference on Robotics and Automation (Cat. No.02CH37292)*, volume 1, pages 248–253 vol.1, 2002.
- [López-Martínez *et al.*, 2015] Javier López-Martínez, José Luis Blanco-Claraco, Daniel García-Vallejo, and Antonio Giménez-Fernández. Design and analysis of a flexible linkage for robot safe operation in collaborative scenarios. *Mechanism and Machine Theory*, 92(C):1–16, 2015.
- [Manti *et al.*, 2016] M. Manti, V. Cacucciolo, and M. Cianchetti. Stiffening in soft robotics: A review of the state of the art. *IEEE Robotics Automation Magazine*, 23(3):93–106, 2016.
- [Murray and Gandhi, 2010] Gabriel Murray and Farhan Gandhi. Multi-layered controllable stiffness beams for morphing: energy, actuation force, and material strain considerations. *Smart Materials and Structures*, 19(4):045002, 2010.
- [Narang *et al.*, 2018] Yashraj S. Narang, Joost J. Vlasak, and Robert D. Howe. Mechanically versatile soft machines through laminar jamming. *Advanced Functional Materials*, 28(17):1707136, 2018.
- [Park *et al.*, 2008] Jung-Jun Park, Byeong-Sang Kim, Jae-Bok Song, and Hong-Seok Kim. Safe link mechanism based on nonlinear stiffness for collision safety. *Mechanism and Machine Theory*, 43(10):1332–1348, 2008.
- [Petit *et al.*, 2010] F. Petit, M. Chalon, W. Friedl, M. Grebenstein, A. Albu-Schäffer, and G. Hirzinger. Bidirectional antagonistic variable stiffness actuation: Analysis, design and implementation. In *2010 IEEE International Conference on Robotics and Automation*, pages 4189–4196, 2010.
- [Petit, 2014] Florian Patrick Petit. *Analysis and control of variable stiffness robots*. Thesis, 2014.
- [Schiavi *et al.*, 2008] R. Schiavi, G. Grioli, S. Sen, and A. Bicchi. Vsa-ii: a novel prototype of variable stiffness actuator for safe and performing robots interacting with humans. In *2008 IEEE International Conference on Robotics and Automation*, pages 2171–2176, 2008.
- [She, 2018] Yu She. *Compliant robotic arms for inherently safe physical human-robot interaction*. Thesis, 2018.
- [Song *et al.*, 2019] Siyang Song, Xianpai Zeng, Yu She, Junmin Wang, and Hai-Jun Su. Modeling and control of inherently safe robots with variable stiffness links. *Robotics and Autonomous Systems*, 120:103247, 2019.
- [Zeng *et al.*, 2020] Xianpai Zeng, Cart Hurd, Hai-Jun Su, Siyang Song, and Junmin Wang. A parallel-guided compliant mechanism with variable stiffness based on layer jamming. *Mechanism and Machine Theory*, 148:103791, 2020.
- [Zhou *et al.*, 2019b] Yitong Zhou, Leon M. Headings, and Marcelo J. Dapino. Discrete Layer Jamming for Variable Stiffness Co-Robot Arms. *Journal of Mechanisms and Robotics*, 12(1), 10 2019b. 015001.
- [Zubrycki and Granosik, 2016] Igor Zubrycki and Grzegorz Granosik. *Novel Haptic Device Using Jamming Principle for Providing Kinaesthetic Feedback in Glove-Based Control Interface*, volume 85. 2016.